Int. J. Heat Mass Transfer. Vol. 27, No. 11, pp. 2067–2075, 1984
Printed in Great Britain

0017-9310/84 $3.00 + 0.00
Pergamon Press Ltd.

Maximum density effects on natural convection in a porous layer differentially heated in the horizontal direction

DIMOS POULIKAKOS

Mechanical Engineering Department, University of Illinois at Chicago, Box 4348, Chicago, IL 60680, U.S.A.

(*Received* 16 *November* 1983 *and in revised form* 16 *February* 1984)

Abstract—This paper reports a fundamental study of natural convection in a fluid saturated porous layer differentially heated in the horizontal direction, when the fluid possesses a density maximum such as that of water at 3.98°C. The study is undertaken in two distinct parts. In the first part the flow and temperature fields in the porous cavity are determined theoretically on the basis of an asymptotic analysis valid in the conduction dominated low Ra regime, where Ra is the Darcy-modified Rayleigh number based on the layer height. It is shown that in this limit the circulation in the porous enclosure consists of two cells, antisymmetric about the midlength. The second part of the study is focused on a complete sequence of numerical simulations covering the ranges $100 \leqslant Ra \leqslant 1000$, $0.5 \leqslant H/L \leqslant 2$, $5 \leqslant T_H \leqslant 7.96$. The numerical solutions prove that increasing the Rayleigh number or decreasing the aspect ratio leads to the development of thermal boundary layers along the two driving walls and the midlength and enhances the role of convection on the net heat transfer across the porous layer. The bicellular flow field, which is a direct result of the existence of the density maximum associated with the temperature of $T_0 = 3.98$°C, is a feature of all the numerical simulations. However, the two cells are antisymmetric about the midlength only in the case where $T_H - T_0 = T_0 - T_C$.

1. INTRODUCTION

BUOYANCY induced flows in fluid saturated porous media have received considerable attention in the recent heat transfer literature, due to the wide recognition of the fact that such flows may drastically influence the heat transfer characteristics of many engineering applications. Some problems of engineering interest whose performance depends on a better understanding of natural convection in porous media are geothermal systems, nuclear reactors, thermal insulations and flows in water-percolated soils.

Natural convection in a porous matrix saturated with cold water is strongly affected by the occurrence of the density extremum associated with the temperature of 3.98°C. At this temperature, the density of water attains a maximum value, thereafter decreasing in a nonlinear manner as the temperature passes the value of 3.98°C hereafter denoted by T_0. This peculiar behavior of cold water density on temperature makes it clear that the usual linear 'Boussinesq' approximation of the temperature effect on density used in conventional analysis must be replaced by another more realistic density–temperature relation, if the phenomenon of buoyancy induced flow in a porous layer saturated with water around T_0 is to be investigated.

Goren [1] and Moore and Weiss [2] showed that for water in the vicinity of T_0 the dependence of density ρ on temperature T_* is parabolic and is given by

$$\Delta\rho = \rho_0\gamma(T_* - T_0)^2 \tag{1}$$

where $(T_* - T_0)$ is not to exceed ± 4°C, and where γ is approximately 8.0×10^{-6}(°C)$^{-2}$.

The free convective motion of an enclosed water body in the region of its maximum density has been the subject of several studies (see for example refs. [3, 4] concerned with natural convection in a rectangular enclosure filled with cold water and differentially heated in the horizontal direction, and ref. [5] which considers the case where a rectangular insulator is cooled from above). However, the problem of natural convection in a cold water-saturated porous enclosure has received considerably less attention. One of the few studies on this topic is the work of Sun and Tien [6] who relied on linear stability analysis to investigate the thermal instability of a horizontal water saturated porous layer around T_0, heated from below. To the author's knowledge the problem of natural convection in a porous layer saturated by water in the vicinity of T_0 and differentially heated in the horizontal direction has not yet been investigated. The study of this problem is the main objective of this paper.

2. MATHEMATICAL FORMULATION

The configuration of interest is shown schematically in Fig. 1. A two-dimensional porous layer of height H and length L is saturated with cold water and bounded by four solid walls. The two vertical walls are maintained at different temperatures, T_H and T_C, respectively ($T_H > T_C$). The two horizontal walls are insulated. The temperatures of the two vertical walls are such that they constitute the upper and the lower bounds of a temperature range which contains the temperature associated with the density maximum in pure water at atmospheric pressure, $T_C < T_0 < T_H$.

According to the homogeneous porous medium

NOMENCLATURE

A	geometric aspect ratio of the porous layer
c_p	fluid specific heat at constant pressure
g	gravitational acceleration
H	height of porous layer
k	thermal conductivity of fluid/porous matrix combination
K	permeability
L	horizontal dimension of porous layer
m	number of vertical grid lines
n	number of horizontal grid lines
Nu	Nusselt number, equation (13)
P	pressure
Q	overall heat transfer
Ra	Darcy-modified Rayleigh number based on H, for a fluid with density extremum, equation (12)
T	temperature
T_C	temperature of cold wall (Fig. 1)
T_0	reference temperature, 3.98°C
T_H	temperature of warm wall (Fig. 1)
u	horizontal velocity component
v	vertical velocity component
x	horizontal Cartesian coordinate
y	vertical Cartesian coordinate.

Greek symbols

α	thermal diffusivity, $k/(\rho c_p)_f$
γ	constant in equation (1)
θ	dimensionless temperature
θ_C	dimensionless cold wall temperature
θ_H	dimensionless warm wall temperature
μ	viscosity
ν	kinematic viscosity
ρ	density
ψ	streamfunction, equations (7) and (8).

Subscript

*	dimensional quantity.

model [7] the 'Boussinesq' equations governing the steady state conservation of mass momentum and energy at each point in the system shown in Fig. 1 are

$$\frac{\partial u_*}{\partial x_*} + \frac{\partial v_*}{\partial y_*} = 0 \tag{2}$$

$$u_* = -\frac{K}{\mu}\frac{\partial P_*}{\partial x_*} \tag{3}$$

$$v_* = -\frac{K}{\mu}\left(\frac{\partial P_*}{\partial y_*} + \rho g\right) \tag{4}$$

$$u_*\frac{\partial T_*}{\partial x_*} + v_*\frac{\partial T_*}{\partial y_*} = \alpha\left(\frac{\partial^2 T_*}{\partial x_*^2} + \frac{\partial^2 T_*}{\partial y_*^2}\right). \tag{5}$$

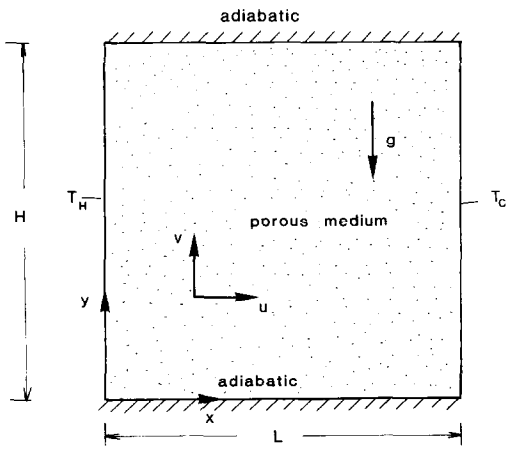

FIG. 1. Schematic of a porous layer saturated with cold water and heated from the side.

In the above equations u_* and v_* are the horizontal and vertical velocity components, x_* and y_* the Cartesian coordinates, T_* the temperature, P_* the pressure, g the gravitational acceleration acting in the negative y_* direction, and μ, ρ the fluid viscosity and density, respectively. The thermal diffusivity α is defined as $\alpha = k/(\rho c_p)_f$, the ratio of the thermal conductivity of the fluid/porous matrix composite k, divided by the fluid thermal capacity $(\rho c_p)_f$. The two momentum equations, equations (3) and (4), are based on the Darcy flow model, where K represents the permeability of the porous material. The fluid and the porous medium are in local thermal equilibrium at temperature T_*.

Before attempting to solve the governing equations, it is convenient to cast them in dimensionless form. Defining the following parameters

$$x = x_*/H, \quad y = y_*/H, \quad u = u_*/(\alpha/H)$$
$$v = v_*/(\alpha/H), \quad \theta = \frac{T_* - T_0}{T_H - T_C} \tag{6}$$

introducing the dimensionless streamfunction ψ

$$u = \frac{\partial \psi}{\partial y}, \quad v = -\frac{\partial \psi}{\partial x} \tag{7,8}$$

eliminating the pressure between equations (3) and (4) and taking into account the parabolic dependence of density on temperature, equation (1), one can rewrite the governing equations (3)–(5) as

$$\nabla^2 \psi = -2Ra\frac{\partial \theta}{\partial x}\theta \tag{9}$$

$$\frac{\partial \psi}{\partial y}\frac{\partial \theta}{\partial x} - \frac{\partial \psi}{\partial x}\frac{\partial \theta}{\partial y} = \nabla^2 \theta. \tag{10}$$

In dimensionless form, the boundary conditions are

$$u = 0, \quad \theta = \theta_H \quad \text{at} \quad x = 0$$
$$u = 0, \quad \theta = \theta_C \quad \text{at} \quad x = A^{-1} \tag{11}$$
$$v = 0, \quad \frac{\partial \theta}{\partial y} = 0 \quad \text{at} \quad y = 0, 1.$$

The boundary conditions account for the impermeability of the four walls which frame the fluid/porous matrix composite and for the fact that the two horizontal walls are adiabatic while the two vertical walls are differentially heated.

In the above equations Ra is the Darcy-modified Rayleigh number appropriate for natural convection in a porous medium saturated by a fluid with density maximum

$$Ra = \frac{Kg\gamma(T_H - T_C)^2 H}{\nu\alpha} \tag{12}$$

and A, θ_H, θ_C the geometric aspect ratio of the cavity ($A = H/L$) and the dimensionless temperatures of the two vertical walls.

The effect of fluid motion on the heat transfer between the two driving vertical walls of the porous layer can be evaluated by computing the conduction-referenced Nusselt number

$$Nu = \frac{Q}{kH(T_H - T_C)/L} \tag{13}$$

where Q is the overall heat transfer rate.

In terms of dimensionless quantities the Nusselt number definition reads

$$Nu = -\frac{1}{A}\int_0^1 \left(\frac{\partial \theta}{\partial x}\right)_{x=0} dy. \tag{14}$$

In what follows equations (9) and (10) are solved subject to boundary conditions (11) and the complete flow and temperature fields in the cavity are determined. The analysis consists of an asymptotic solution for the conduction-dominated low Ra regime and a series of numerical solutions of the full governing equations.

3. LOW RAYLEIGH NUMBER REGIME

Solutions for the low Rayleigh number regime can be obtained in terms of asymptotic expansions in Ra of the unknown variables of the problem, ψ and θ

$$\psi = \psi_0 + Ra\ \psi_1 + Ra^2\ \psi_2 + \cdots \tag{15}$$
$$\theta = \theta_0 + Ra\ \theta_1 + Ra^2\ \theta_2 + \cdots \tag{16}$$

Substituting equations (15) and (16) into expressions (9) and (10) and equating terms of equal order in Ra yields a sequence of linear equations for the successive ψ_1, θ_1, ψ_2, θ_2... It can be easily shown that the zero-order solutions are

$$\psi_0 = 0 \tag{17}$$
$$\theta_0 = -A^{-1}x + \theta_H. \tag{18}$$

Hence, the expansion is about the pure conduction mode. The first-order equations read

$$\nabla^2\psi_1 = -2\theta_0 \frac{\partial \theta_0}{\partial x} \tag{19}$$

$$\nabla^2\theta_1 = \frac{\partial \psi_0}{\partial y}\frac{\partial \theta_1}{\partial x} + \frac{\partial \psi_1}{\partial y}\frac{\partial \theta_0}{\partial x} - \frac{\partial \psi_0}{\partial x}\frac{\partial \theta_1}{\partial y} - \frac{\partial \theta_0}{\partial y}\frac{\partial \psi_1}{\partial x}. \tag{20}$$

By using the modified Garlekin method [8] the above Poisson equations are reduced to ordinary differential equations. Omitting the details of the procedure, since they can be found in ref. [8] among others, only the main results are reported here.

The final expression for ψ_1 is

$$\psi_1(x,y) = \left\{-\frac{A^{-2}}{3}x^3 + \theta_H A^{-1}x^2 + \left(\frac{A^{-4}}{3} - \theta_H A^{-2}\right)x\right\} \times \{\sinh[\lambda^{1/2}(y-1)] - \sinh(\lambda^{1/2}y) + \sinh\lambda^{1/2}\}/\sinh\lambda^{1/2} \tag{21}$$

where

$$\lambda = \frac{3A^{-4}/11.25 - \theta_H A^{-2} - \theta_H^2}{3A^{-6}/118.25 - \theta_H A^{-4}/10 + \theta_H^2 A^{-2}/10}. \tag{22}$$

Similarly, the solution for θ_1 reads

$$\theta_1(x,y) = \left\{\frac{A^{-3}}{60}x^5 - \frac{\theta_H A^{-2}}{12}x^4 + \left(-\frac{A^{-5}}{18} + \frac{\theta_H A^{-3}}{6}\right)x^3 - \left(-\frac{21A^{-7}}{540} + \frac{\theta_H A^{-5}}{12}\right)x\right\}\left\{\left(\frac{\lambda}{\xi}\right)^{1/2} \times (\cosh[\xi^{1/2}(y-1)] - \cosh(\xi^{1/2}y))/\sinh\xi^{1/2} - (\cosh[\lambda^{1/2}(y-1)] - \cosh(\lambda^{1/2}y))/\sinh\lambda^{1/2}\right\}\frac{\lambda\xi}{\lambda - \xi} \tag{23}$$

where

$$\xi = \frac{-\theta_H A^{-2} + 0.251A^{-4} + \theta_H^2}{-\theta_H A^{-4}/9.871 + A^{-6}/39.446 + \theta_H^2 A^{-2}/9.871}. \tag{24}$$

Although obtaining solutions beyond the first order is straightforward, the analysis is not carried further because the algebra becomes very tedious.

The perturbation solutions ψ_1, θ_1 are illustrated graphically in Fig. 2 for an aspect ratio $A = 1$. The streamline map shown in Fig. 2(a) proves that the linear temperature profile of the pure conduction regime θ_0 [equation (18)], induces a flow pattern which consists of two identical cells: the left rotating clockwise and the right rotating counterclockwise. Hence, ψ_1 is antisymmetric with respect to the midlength (negative in the left half and positive in the right half of the porous layer). In addition, ψ_1 is symmetric with respect to the midheight of the cavity. Figure 2(b) shows that θ_1 is antisymmetric

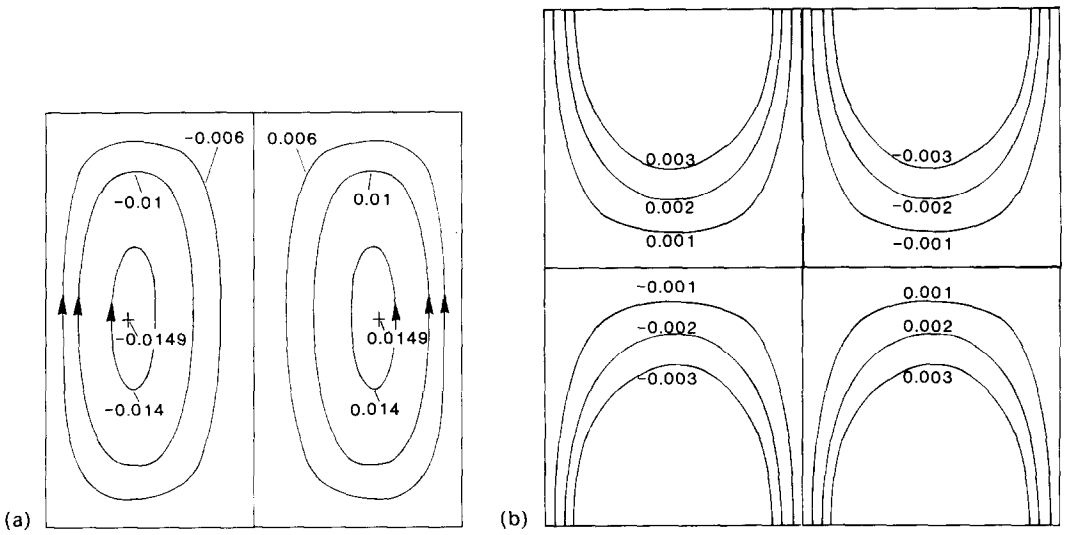

FIG. 2. Results of the first-order asymptotic solution: $A = 1, T_H = 7.96°C, T_C = 0°C$. (a) Streamline pattern, ψ_1. (b) Isotherm pattern, θ_1.

with respect to both the midheight and the midlength of the porous layer. The behavior of ψ_1 and θ_1 indicates that, in the left half of the enclosure, the fluid traveling upward along the solid wall, removes heat from the wall effectively only in the lower half of the layer. In the upper half, the fluid is already warm and cannot remove heat from the wall effectively, therefore, the temperature rises above the pure conduction limit. Analogous conclusions can be drawn by looking at the shape of ψ_1 and θ_1 in the right half of the porous layer. Finally, since θ_1 is antisymmetric about the midheight, it is clear that θ_1 does not contribute to the calculation of the Nusselt number [equation (14)]. Hence, the perturbation analysis is valid only in the case where the heat transfer across the porous enclosure is conduction dominated.

4. NUMERICAL SOLUTION

The discretized form of the governing equations and boundary conditions (9)–(11) was obtained by overlaying the region of interest with m vertical and n horizontal grid lines spaced equidistantly in both the x- and y-directions, and by using the control volume formulation [9]. The grid fineness $m = n = 33$ was used for the case $A = 1$ throughout this study even though $m = n = 21$ yielded satisfactory results. The grids used for the various runs in the course of the present study are listed in Table 1.

The power law scheme, introduced, tested and recommended by Patankar [9] was employed to obtain the temperature field from equation (10). The streamfunction was calculated earlier from equation (9) by using the successive over-relaxation method [9, 10] and a known temperature distribution. The process was repeated until convergence was obtained. The final temperature and flow fields satisfied the following criterion

$$\frac{\sum_{i=1}^{m}\sum_{j=1}^{n}|\phi_{i,j}^{r+1}-\phi_{i,j}^{r}|}{\sum_{i=1}^{m}\sum_{j=1}^{n}|\phi_{i,j}^{r+1}|} < 10^{-6} \tag{25}$$

where ϕ refers to θ or ψ and r denotes the number of iterations.

The conduction referenced Nusselt number was evaluated by integrating equation (14) numerically after the final temperature field was obtained. It is worth noting that a relation analogous to equation (14) can be obtained by integrating the heat flux along the right wall of the porous layer, situated at $x = A^{-1}$. This second Nusselt number was also calculated as a check

Table 1

Ra	A	T_H(°C)	Nu	Grid fineness ($m \times n$)
10^3	1	5	10.24	33 × 33
10^3	1	6	7.48	33 × 33
10^3	1	7	5.22	33 × 33
10^3	1	7.96	4.157	33 × 33
900	1	7.96	3.98	33 × 33
800	1	7.96	3.75	33 × 33
700	1	7.96	3.51	33 × 33
600	1	7.96	3.1	33 × 33
500	1	7.96	2.704	33 × 33
400	1	7.96	2.31	33 × 33
300	1	7.96	1.948	33 × 33
200	1	7.96	1.49	33 × 33
100	1	7.96	1.172	33 × 33
10^3	0.5	7.96	6.97	65 × 33
10^3	1.5	7.96	2.65	33 × 49
10^3	2	7.96	1.76	33 × 65

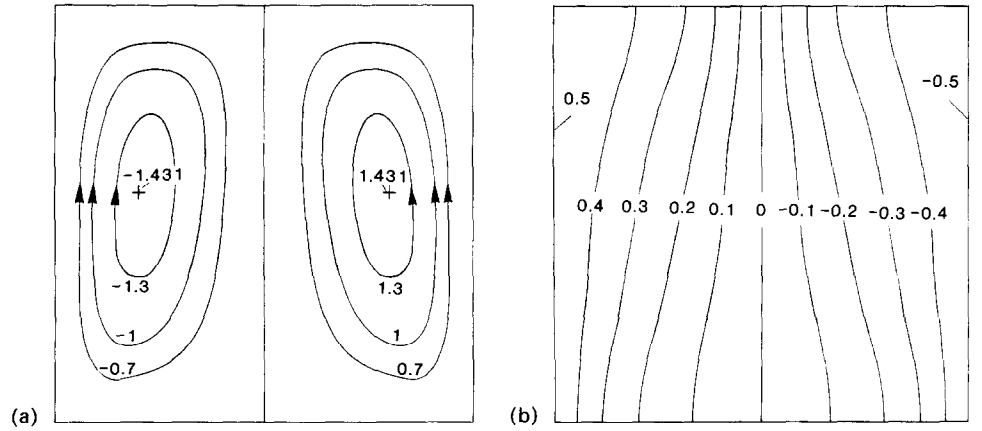

FIG. 3. Numerical results for $Ra = 100$, $A = 1$, $T_H = 7.96°C$, $T_C = 0°C$. (a) Streamline pattern. (b) Isotherm pattern.

and the results were found to be nearly identical to the values yielded by equation (14) (the error was less than 3% throughout this study).

5. RESULTS AND DISCUSSION

The numerical simulations were carried out systematically in order to determine the effect of the three main parameters of the problem, namely: the Rayleigh number Ra, the aspect ratio A and the temperature of the left wall T_H, on the flow and temperature fields in the porous layer. The temperature of the right wall was held constant at $T_C = 0°C$ ($\theta_C = -0.5$) throughout the present study.

5.1. *The effect of Rayleigh number*

Figures 3 and 4 show the streamline and temperature fields in a system with fixed aspect ratio $A = 1$ and left wall temperature $T_H = 7.96°C$ ($\theta_H = 0.5$). The value of the Rayleigh number increases from $Ra = 100$ in Fig. 3 to $Ra = 1000$ in Fig. 4. The streamline pattern in both cases consists of two counter-rotating symmetric cells [Figs. 3(a) and 4(a)]. This result underlines the drastic effect of the density maximum associated with temperature T_0 on the resulting flow field. Note that the counterpart of the present study, for temperature regions in which the density does not possess an extremum, i.e. temperature regions in which the usual 'Boussinesq' linear density–temperature relationship is appropriate, exhibits a unicellular flow pattern [11, 12]. As shown in Figs. 3(a) and 4(a), increasing the Rayleigh number strengthens the bicellular flow and shifts the locations of the steamfunction extrema towards the cross-section of the top wall and the line of symmetry at $x_* = L/2$. The effect of this 'strengthening' of the flow is reflected on the resulting temperature fields, Figs. 3(b) and 4(b), which illustrate how the heat transfer mode across the porous layer transforms from conduction dominated. [Fig. 3(b), $Ra = 100$] to thermal boundary layer convection dominated [Fig. 4(b), $Ra = 1000$]. The temperature fields are also antisymmetric about the midlength. A summary of heat transfer results is

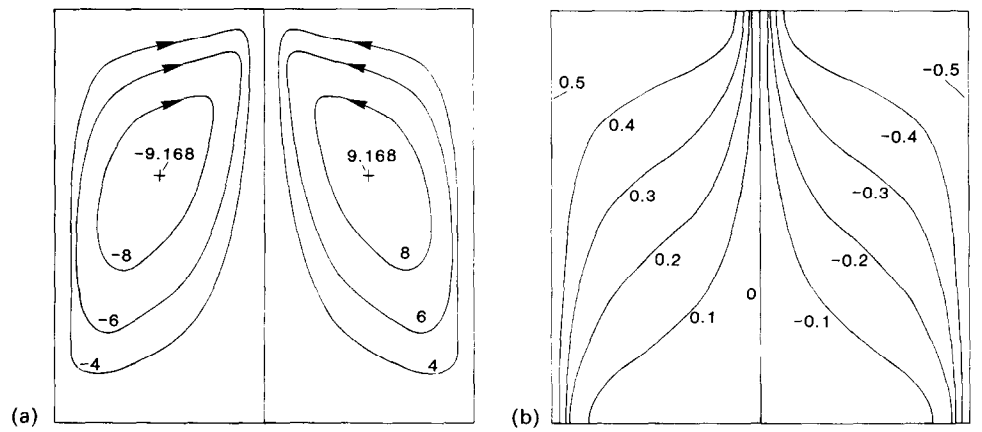

FIG. 4. Numerical results for $Ra = 1000$, $A = 1$, $T_H = 7.96°C$, $T_C = 0°C$. (a) Streamline pattern. (b) Isotherm pattern.

shown in Fig. 7 by means of a Nu vs Ra graph. This graph indicates that for $Ra < 100$ the net heat transfer across the porous layer is almost identical to the pure conduction limit. The importance of convection increases monotonically with Ra. The values of Nu shown graphically in Fig. 7, are tabulated in Table 1.

5.2. *The effect of aspect ratio*

During this series of numerical simulations the warm wall temperature and the Rayleigh number were kept fixed, $T_H = 7.96°C$ and $Ra = 1000$. Figure 5 shows the streamline and temperature patterns in a shallow porous layer ($A = 0.5$). As in the flows exhibited earlier for a square enclosure ($A = 1$), the streamline pattern consists of two counter-rotating cells [Fig. 5(a)] and the temperature field is antisymmetric about the midlength [Fig. 5(b)]. The sharp thermal boundary layers existing along the vertical walls and the midlength and the almost horizontal shape of the isotherms outside these boundary layers, indicate a considerably stronger convection effect on heat transfer than the effect observed earlier for a square layer (Fig. 4). The fact that decreasing the aspect ratio enhances the role of convection is also illustrated by the respective values of Nu in Fig. 7 and Table 1. The flow and temperature fields in a relatively tall system ($A = 2$) exhibit similar characteristics with the previous cases, hence, they are omitted here for brevity. However, Fig. 7 and Table 1 reveal that increasing the aspect ratio of the layer enhances conduction and decreases the value of the Nusselt number.

5.3. *The effect of warm wall temperature*

This part of the study is aimed toward determining the effect of 'asymmetric' heating of the porous layer on the resulting flow and temperature fields. To isolate this effect the Rayleigh number and the aspect ratio were kept constant at $Ra = 1000$ and $A = 1$ throughout this part of the numerical investigation. The streamline and isotherm maps shown in Fig. 6, exhibit a striking difference relative to the findings in Figs. 3–5. The flow field still consists of two counter-rotating cells, however, the right cell is much stronger than the left cell, and, as a result, it forces the left cell into the neighborhood of the lower left corner. This is a direct result of the fact that the heating effect of the left wall ($T_H = 5°C$) is weaker than the cooling effect of the right wall ($T_C = 0°C$); hence, the porous layer is primarily

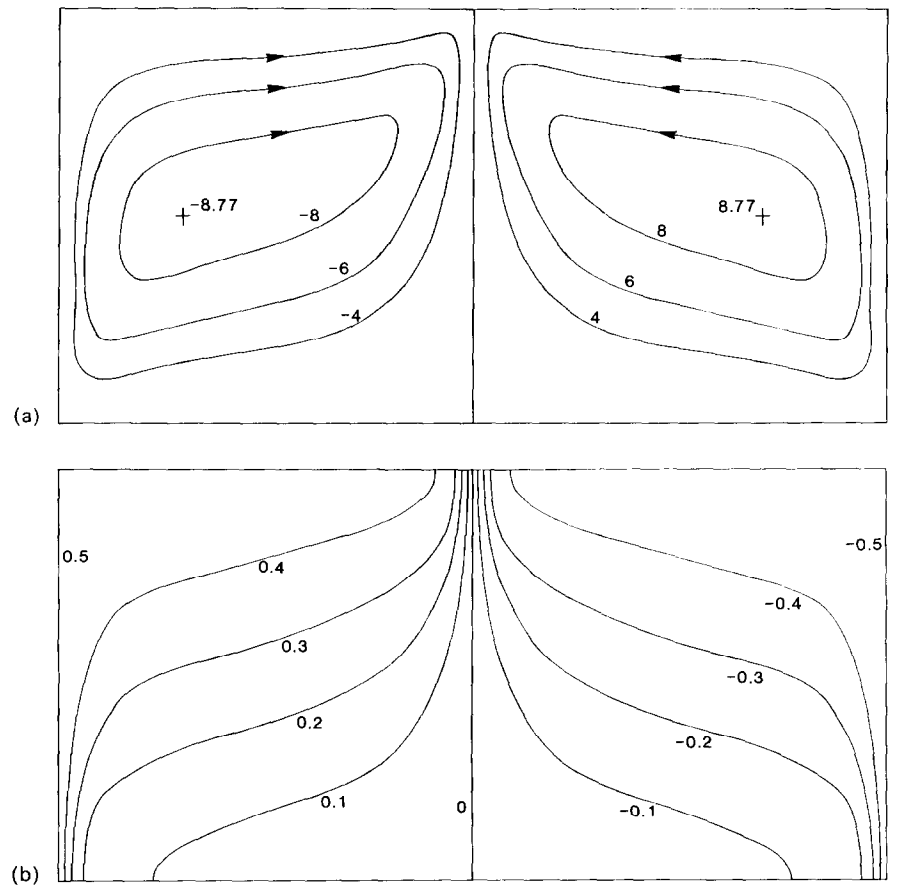

FIG. 5. Numerical results for $Ra = 1000$, $A = 0.5$, $T_H = 7.96°C$, $T_C = 0°C$. (a) Streamline pattern. (b) Isotherm pattern.

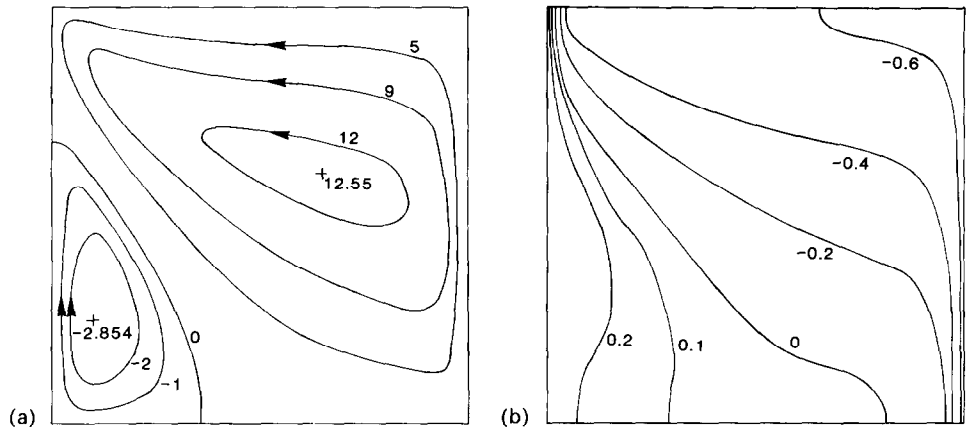

FIG. 6. Numerical results for $Ra = 1000$, $A = 1$, $T_H = 5°C$, $T_C = 0°C$. (a) Streamline pattern. (b) Isotherm pattern.

occupied by cold fluid [Figs. 5(a) and (b)]. The fact that the cold fluid finds direct access to the warm wall has a drastic effect on the heat transfer through the enclosure. Witness to this event, the values of Nu in Fig. 7 and Table 1 exemplified by $T_H = 5°C$ which yields $Nu = 10.29$ (Fig. 7 and Table 1). This value is approximately 2.5 times larger than the value of Nu corresponding to the case of symmetric side heating and cooling ($T_H = 7.98$, $Nu = 4.157$).

5.4. *Numerical verification of the asymptotic theory of Section 3*

In order to obtain an estimate regarding the range of validity of the analytical results developed in Section 3, a number of numerical calculations were conducted for the streamfunction profile in the vertical plane $x_* = L/4$, for $A = 1$ and for a range of Rayleigh numbers. As shown in Fig. 8, the asymptotic theory predicts the flow accurately provided that $Ra < 0.1$. In addition, the agreement is acceptable for $Ra < 1$. Note that for $Ra = 1$, the theoretical streamfunction predicts to within 3% the numerical results.

6. CONCLUSIONS

This study examined the heat transfer and fluid flow characteristics of natural convection in a porous layer saturated with water around T_0 when the layer is differentially heated in the horizontal direction. It was found that the low Ra regime is accurately predicted by a perturbation solution if $Ra < 0.1$ (Fig. 8). The analytical solution gives also satisfactory results for $0.1 < Ra < 1$ (Fig. 8). The full equations were solved numerically and it was concluded that the density extremum is responsible for a bicellular flow pattern in the enclosure. The two cells are counter-rotating but their relative size and shape greatly depends on the temperature of the warm wall, if the temperature of the cold wall is held fixed [Figs. 3(a) and 6(a)]. The relative size of the two cells has a drastic effect on the net heat transfer across the layer, i.e. heating and cooling the porous layer asymmetrically through its two vertical

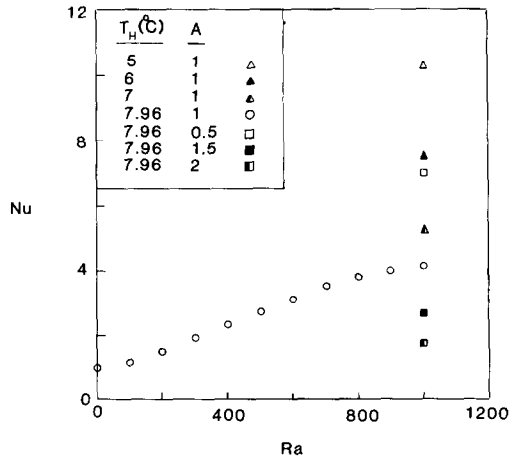

FIG. 7. The dependence of Nu on the parameters of the problem (Ra, A, T_H).

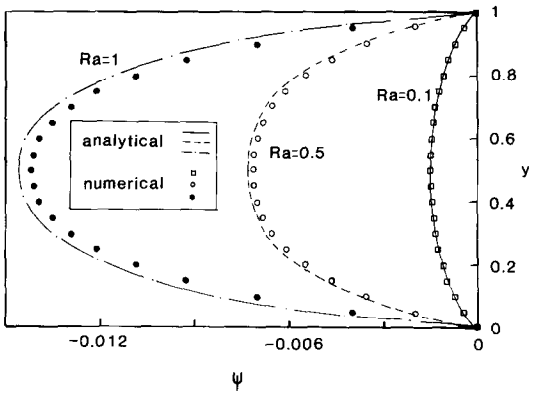

FIG. 8. Comparison of numerical and analytical results. Streamfunction profiles at $x_* = L/4$.

walls significantly enhances the net heat transfer across the cavity (Fig. 7 and Table 1). The geometric aspect ratio of the enclosure seriously affects the temperature field in the cavity. Witness to this event the fact that decreasing the aspect ratio from $A = 2$ to 0.5 transformed the temperature field from conduction dominated to thermal boundary layer convection dominated [Figs. 5(b) and 7 and Table 1]. Summarizing, the simple geometry of a porous layer saturated with water in the vicinity of its density maximum and heated from the side, results in a variety of natural convection flows depending on Ra, A and the relative size of $T_H - T_0$ and $T_0 - T_c$.

REFERENCES

1. S. L. Goren, On free convection in water at 4°C, *Chem. Engng Sci.* **21,** 515–518 (1966).
2. D. R. Moore and N. O. Weiss, Nonlinear penetrative convection, *J. Fluid Mech.* **61,** 553–581 (1973)
3. V. S. Desai and R. E. Forbes, *Environ. Geophys. Heat Transfer* **4,** 41 (1971).
4. A. Watson, The effect of the inversion temperature on the convection of water in an enclosed rectangular cavity, *Q. J. Mech. Appl. Math.* **20,** 423–446 (1972).
5. R. E. Forbes and J. W. Cooper, Natural convection in a horizontal layer of water cooled from above to near freezing, *Trans. Am. Soc. Mech. Engrs*, Series C, *J. Heat Transfer* **97,** 47–53 (1975).
6. Z. S. Sun and C. Tien, Onset of convection in a porous medium containing liquid with a density maximum, *Heat Transfer 1970*, Vol. 4, pp. 160–165 (1982).
7. P. Cheng, Heat transfer in geothermal systems, *Adv. Heat Transfer* **14,** 1–105 (1979).
8. S. G. Miklin, *Variational Methods in Mathematical Physics*. Macmillan, New York (1964).
9. S. Patankar, *Numerical Heat Transfer and Fluid Flow*, Hemisphere, New York (1980).
10. P. J. Roache, *Computational Fluid Dynamics*. Hermosa, Albuquerque, New Mexico (1976).
11. C. E. Hickox and D. K. Gartling, A numerical study of natural convection in a horizontal porous layer subjected to an end-to-end temperature difference, *Trans. Am. Soc. Mech. Engrs*, Series C, *J. Heat Transfer* **103,** 797–802 (1981).
12. D. Poulikakos and A. Bejan, Unsteady natural convection in a porous layer, *Physics Fluids* **26,** 1183–1191 (1983).

EFFETS DU MAXIMUM DE DENSITE SUR LA CONVECTION NATURELLE DANS UNE COUCHE HORIZONTALE CHAUFFEE DIFFERENTIELLEMENT DANS LA DIRECTION HORIZONTALE

Résumé—On étudie fondamentalement la convection naturelle dans une couche poreuse saturée et chauffée différentiellement dans la direction horizontale, quand le fluide présente un maximum de densité comme l'eau à 3,98°C. L'étude est conduite en deux parties distinctes. Dans la première, les champs de vitesse et de température sont déterminés théoriquement à partir d'une analyse asymptotique valable dans le cas du régime de faibles Ra, où Ra est le nombre de Rayleigh-modifié Darcy et basé sur la hauteur de la couche. On montre que pour cette limitation, la circulation dans le volume poreux concerne deux cellules, antisymétrique autour du plan médian. La seconde partie de l'étude est centrée sur une séquence complète de simulations numériques qui convient aux domaines $100 \leqslant Ra \leqslant 1000$, $0{,}5 \leqslant H/L \leqslant 2$, $5 \leqslant T_H \leqslant 7{,}96$. Les solutions numériques prouvent que l'augmentation du nombre de Rayleigh, ou la diminution du rapport de forme, conduit au développement des couches limites thermiques le long des deux parois et le milieu et augmente le rôle de la convection sur le transfert de chaleur à travers la couche poreuse. Le champ d'écoulement bicellulaire qui est un résultat direct de l'existence du maximum de densité associé à la température $T_0 = 3{,}98$°C, est ufe configuration de toutes les simulations numériques. Néanmoins les deux cellules sont antisymétriques autour de la ligfe médiane dans le cas où $T_H - T_0 = T_0 - T_C$.

EINFLÜSSE EINES DICHTEMAXIMUMS AUF DIE NATÜRLICHE KONVEKTION IN EINER PORÖSEN, IN HORIZONTALER RICHTUNG UNTERSCHIEDLICH ERWÄRMTEN SCHICHT

Zusammenfassung—In dieser Arbeit wird über Grundlagenuntersuchungen zur natürlichen Konvektion in einer mit einem Fluid gesättigten Schicht berichtet, die in horizontaler Richtung unterschiedlich erwärmt wird, wobei das Fluid ein Dichtemaximum so wie Wasser bei 3,98°C aufweist. Die Untersuchung gliedert sich in zwei Teile. Im ersten Teil werden die Strömungs- und Temperaturfelder in dem porösen Raum theoretisch auf der Basis einer Reihenentwicklung für den durch Wärmeleitung bestimmten Bereich geringer Rayleigh-Zahl bestimmt. Dabei ist Ra die nach Darcy modifizierte Rayleigh-Zahl mit der Schichthöhe als Bezugsgröße. Es zeigt sich, daß in diesem Bereich die Zirkulation in dem porösen Raum aus zwei zur Mittellinie asymmetrischen Zellen besteht. Der zweite Teil der Untersuchung betrifft eine komplette Folge numerischer Simulationen, die folgende Bereiche abdecken: $100 \leqslant Ra \leqslant 1000$; $0{,}5 \leqslant H/L \leqslant 2$ und $5 \leqslant T_H \leqslant 7{,}96$. Die numerischen Lösungen zeigen, daß eine Zunahme der Rayleigh-Zahl oder eine Abnahme des Seitenverhältnisses zur Entwicklung thermischer Grenzschichten an den beiden treibenden Wänden und der Mittellinie führt und den Anteil der Konvektion an der Nettowärmeübertragung durch die porösen Schicht erhöht. Das bizellulare Strömungsfeld, welches sich direkt aus dem Vorhandensein des Dichtemaximums bei der Temperatur von $T_0 = 3{,}98$°C ergibt, ist ein charakteristisches Merkmal aller numerischen Simulationen.

Die beiden Zellen sind jedoch nur dann zur Mittellinie antisymmetrisch, wenn $T_H - T_0 = T_0 - T_C$ ist.

ВЛИЯНИЕ МАКСИМУМА ПЛОТНОСТИ НА ЕСТЕСТВЕННУЮ КОНВЕКЦИЮ В ПОРИСТОМ СЛОЕ ПРИ НЕРАВНОМЕРНОМ ПОДОГРЕВЕ В ГОРИЗОНТАЛЬНОМ НАПРАВЛЕНИИ

Аннотация—Проведено фундаментальное исследование естественной конвекции в насыщенном жидкостью пористом слое при неравномерном в горизонтальном направлении подогреве в случае, когда жидкость имеет такой же максимум плотности, как вода при 3,98 С. Исследование состоит из двух частей. В первой части поля скоростей и температур в пористом слое определяются теоретически на основе асимптотического анализа режима, в котором при малых значениях числа Ra преобладает теплопроводность, где Ra—Дарси-модификация числа Рэлея, основанного на высоте пористого слоя. Показано, что в этом случае жидкость циркулирует в слое в виде двух ячеек, несимметричных относительно середины длины слоя. Во второй части работы проведено численное моделирование в следующих диапазонах: $100 \leq Ra \leq 1000$, $0{,}5 \leq H/L \leq 2$, $5 \leq T_{\text{н}} \leq 7{,}96$. Результаты численных решений показывают, что в результате увеличения значения числа Рэлея или уменьшения отношения сторон происходит развитие тепловых пограничных слоев вдоль двух охлаждаемых стенок и в середине длины слоя и возрастает роль конвекции в результирующем переносе тепла поперек слоя. Поле двухячеистого течения, развивающееся в связи с наличием максимума плотности при температуре $T_0 = 3{,}98$ С, является характерным для всех численных моделей. Однако, только в случае, когда $T_{\text{н}} - T_0 = T_0 - T_{\text{с}}$, две ячейки являются несимметричными относительно середины длины.